Ground vibration measurements for Fermilab future collider projects

B. Baklakov, T. Bolshakov, A. Chupyra, A. Erokhin, P. Lebedev, V. Parkhomchuk, and Sh. Singatulin
Budker Institute of Nuclear Physics, Novosibirsk 630090, Russia

J. Lach and V. Shiltsev*
Fermi National Accelerator Laboratory, Batavia, Illinois 60510
(Received 28 April 1998; published 13 July 1998)

This article presents results of wideband seismic measurements at the Fermilab site, namely, in the tunnel of the Tevatron and on the surface nearby, as well as in two deep tunnels in the Illinois dolomite, thought to be a possible geological environment of the Fermilab future accelerators. [S1098-4402(98)00009-3]

PACS numbers: 41.75.–i, 29.27.–a, 91.30.Dk

I. INTRODUCTION

Ground motion can cause significant deterioration of large future collider operation, due to the vibration of numerous focusing magnets leading to beam emittance growth and beam orbit oscillations. Recently, a series of alignment and vibration studies concerning the stability of future accelerator facilities such as photon and meson factories, future linear e^+e^- colliders, and hadron supercolliders has been carried out (see, e.g., reviews [1,2] and references therein). There are several future collider projects under consideration at Fermilab, including muon collider (MC) [3], linear collider (LC), and very large hadron collider (VLHC) [4]. Although the ground motion effects are different, on site data on seismic vibration are of interest for all of them.

In the muon collider, where $\mu^+\mu^-$ beams live just several hundred turns, vibrations of the strong final focus quadrupoles will lead to off-center collisions at the interaction point. This is of concern because of the very small transverse beam size (<3 μm).

Similar effects exist in the linear collider, too; here, all quadrupoles in two linacs can contribute. It makes tolerances on differential quadrupoles motion more stringent. At low frequency the beam can be used in a feedback loop to keep the bunches colliding by using steering magnets, but at frequencies greater than about 1/20th of the linac repetition frequency, this becomes very difficult. In addition, depending on the beam parameters, nonstraight beam trajectory distorted by displaced quadrupoles may lead to an increase of the transverse emittance during acceleration.

Besides concerns about orbit stability, operation of large hadron colliders is a potential subject of transverse emittance growth due to fast (turn-to-turn) dipole angular kicks $\delta\theta = \sigma_q/F$ produced by the fast motion of quadrupoles. The emittance growth rate [5] is

$$d\epsilon_N/dt = (1/2)\gamma N_q f_0^2 \overline{\beta} S_{\delta\theta}(\Delta\nu f_0), \qquad (1)$$

where f_0 is the revolution frequency, γ is the relativistic factor, $\Delta\nu$ is a fractional part of tune, $S_{\delta\theta}(f)$ is the power spectrum density of kick at a quadrupole $\delta\theta$, F is the focal length of the quadrupole, N_q is a total number of quadrupole focusing magnets, and $\overline{\beta}$ is the mean beta function. Larger accelerator ring circumference leads to smaller revolution frequency, and, e.g., for the VLHC, 90–230 Hz vibrations are of particular concern as they resonate with the beam betatron frequency $\Delta\nu f_0$. For example, for a white seismic noise with rms value of magnet vibrations σ_q, one gets

$$d\epsilon_N/dt \simeq (1/2) f_0 \gamma \overline{\beta} N_q (\sigma_q/F)^2. \qquad (2)$$

If one requires the emittance increase during the luminosity lifetime τ_L to be less than 10% of the initial emittance ϵ_N, the resulting limit on the turn-by-turn ground noise amplitude is extremely small, approximately a few atomic sizes.

Table I shows the main parameters of the three collider projects and their tolerances on low frequency vibrations taken from [2,6,7]. The comparison of the amplitude tolerances σ_q with the results of measurements worldwide (see Sec. V below) shows that for all these colliders the ground vibrations may lead to severe consequences.

This article is devoted to ground motion measurements that were carried out in August–October 1997 and covered almost five decades in frequency from 0.01 to 450 Hz. In Sec. II we briefly describe the seismic probes we used and our procedures and data acquisition system. In Sec. III we present results of surface measurements at Fermilab. Deep tunnel measurement results are presented in Sec. IV. Finally, a brief overview and conclusions are given in Sec. V.

*Corresponding author. Also at Budker INP, Novosibirsk 630090, Russia.

TABLE I. Future colliders: parameters and vibration tolerances.

Parameter	VLHC	MC	LC
Beam energy E (TeV)	50	0.25−2	0.25
Circumference C (km)	550	1−7	8
Norm. emittance ϵ_N (μm rms)	1	50	0.05
$\mathcal{L}$ -lifetime τ_L	5 h	10^3 turns	—
Collision f_0 (kHz)	0.54	0.43−3	0.18
$f_1 = \Delta\nu f_0$ or $f_{\rm rep}/20$ (Hz)	90−230	—	6
Jitter limit σ_q at $\geq f_1$ (nm rms)	0.3	100	5
Measured σ_q (nm rms)	0.1−50	10−1000	1−30

II. SEISMIC PROBES AND DATA ACQUISITION SYSTEM

The data acquisition system used an IBM PC Pentium 200 computer and two seismic stations. Each station consists of a set of probes and a data acquisition (DAS) module. The backbone of our seismic instrumentation is a modified geophone of SM3-KV type, made by the collaboration of the Special Design Bureau of the Institute of Earth Physics (Moscow) and Budker INP (Novosibirsk). The SM3-KV seismometer is a single pendulum velocity meter designed to measure (by choice) either the vertical or the horizontal vibration component in the frequency range from 0.07 to 120 Hz. Supplemental data on the ground motion were obtained with two triaxial very broad band STS-2 seismometers (Streckeisen AG, Switzerland) and two W-731A seismic accelerometers (Wiloxon Research, Maryland). The main parameters of these probes are presented in Table II.

To be sure of the results of the measurements, one needs to evaluate the signal-to-noise ratio of seismic probes. Figure 1 presents typical power spectral densities of the ground motion at the rather quiet deep tunnel of the Tunnel and Reservoir Project (TARP) (see below), measured by the SM3-KV probe, and noise of the probe if its pendulum is fixed. One can see that the signal-to-noise ratio exceeds 6 dB at low frequency of about 0.05 Hz and at high frequency of 130−200 Hz. Similar conclusions can be made from correlation measurements with two SM3-KV seismometers installed side by side. For comparison, Fig. 1 shows equivalent noise due to electronics and cables only, i.e., the probe was

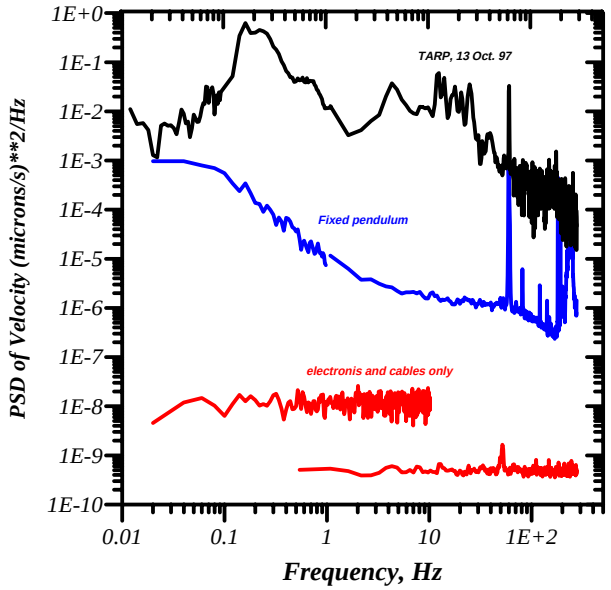

FIG. 1. (Color) Power spectral densities of vertical ground velocity measured by the SM3-KV probe in quiet condition (upper line), the same with fixed pendulum (middle), and equivalent noise of electronics only (two lower curves).

disconnected from the DAS module preamplifier. Two curves correspond to the rms noise value of 0.5 nm/s with sampling frequencies of 25 and 554 Hz.

The seismic probes are connected to the stations by short 5 m long cables. A maximum of eight analog signals can be processed by the DAS module of each station. The stations can be installed at a relatively large distance because they are connected to the PC operation board by a single RG58 cable up to 300 m long. Usually we supply each station with 24 V and about 1.2 A of dc power through additional coaxial cable.

By a command from the PC, we can change gain and low-pass filters of the DAS module amplifiers and sampling frequency. To suppress a frequency "aliasing" usual for digital Fourier transformation, we use analog 4th order Butterworth low-pass filters with 3 dB frequencies of 2, 20, 200, and 2000 Hz. Gain can be changed from 1 to 30. Sample frequencies vary from 2 to 700−900 Hz.

The software to process data delivered to the PC operation board is written on C++ for Windows'95. It provides access to DAS module sample frequency, filter, and gain

TABLE II. Seismic probes.

Probe	SM-3KV	STS-2	W-731A
Sensitivity	0.083 $\frac{\rm V}{\mu\rm m/s}$	0.0015 $\frac{\rm V}{\mu\rm m/s}$	10^{-6} $\frac{\rm V}{\mu\rm m/s^2}$
Output	velocity	velocity	acceleration
Range (Hz)	0.07−120	0.005−15	10−400
Sensors	1 inductive	3 capacitive	1 piezo
Mass (kg)	≃8	13	0.5
Size (cm)	24 × 17 × 14.5	23.5 diam. × 26	6.2 diam. × 5
T range (°C)	−10 to ±45	−5 to ±65	0 to ±40

for each channel. Probe signals and spectra can be displayed on the PC monitor on-line and/or stored on a hard disk.

For any pair of the stationary random processes $x(t)$ and $y(t)$, the correlation spectrum $S_{xy}(f)$ is defined as a limit $T \to \infty$ of

$$S_{xy} = \frac{2}{T}\int_0^T x(t)e^{i\omega t}\,dt \int_0^T y(t)e^{-i\omega t}\,dt\,, \qquad (3)$$

where T is the time of measurement and $\omega = 2\pi f$ is the frequency. Power spectral density (PSD) $S_x(f)$ of signal $x(t)$ is equal to $S_{xx}(f)$. Normalized correlation spectrum (which we quote below) is defined as

$$C_{xy}(f) = \frac{\langle S_{xy}\rangle}{\sqrt{\langle S_{xx}\rangle\langle S_{yy}\rangle}}\,, \qquad (4)$$

where $\langle \ldots \rangle$ means an averaging over a series of measurements with finite T.

By definition, $C_{xy}(f)$ is a complex function. The modulus of the correlation $|C(f)_{xy}|$ is the coherence of two signals at frequency f, $0 \le |C(f)_{xy}| \le 1$. For example, if $C_{xy}(f) = 0$ then the Fourier components of the signals are not related, i.e., the phase difference between them varies in time.

During our measurements we used 1024-point fast Fourier transformation (FFT) of data from 16 channels of both stations to calculate the PSDs $S_{1\cdots16}(f)$ and the correlation spectra matrix $C_{xy}(f)$. To reduce statistical errors in the spectra estimate, we averaged the spectra up to several hundred times.

Figure 2 shows a typical setup configuration used for measurements in the Tevatron tunnel. Here, SM3 are the SM3-KV probes (V-vertical and H-horizontal), piezo is the piezoaccelerometer, BPM and BLM are beam position monitor and beam loss monitor, respectively.

III. MEASUREMENTS AT FERMILAB

Initial measurements and tests of seismic equipment have been carried out on the surface at the E4 location (building E4R, southwest corner of the Fermilab main ring) near the Tevatron radiofrequency (RF) building. To characterize the general seismic conditions at the place of the measurements, we made a long time run with 5 Hz sampling frequency and 2 Hz low-pass filter. The sampling frequency was limited by the computer hard drive capacity (higher rates lead to excessive memory needed for the same time record). Figure 3 presents the record of the maximum vertical ground velocity amplitude in a two-and-a-half-day time scale. One can see a significant increase of the signal from 7:30 a.m. to 2:00 p.m. on Saturday, September 6, 1997, due to construction activities at the Fermilab main injector, traffic noise, and operation of equipment within a few kilometers from the detector. It is interesting to note a drop of activity at lunch time (about 11:00 a.m.). Saturday afternoon and Sunday are seismically quiet with the amplitude some 10 times less than that at working time. Operations resumed Monday morning at 7:00 a.m.

Figure 4 illustrates ground motion under quiet conditions at E4R. It shows signals of two SM3-KV geophones separated by 32 m on the night of September 17, 1997.

Both signals are similar and 5–7 s period oscillations are clearly seen. It is well known that this "7 s hum" of microseismic waves with some dozens of kilometers of wavelength is produced at the nearest coasts and can be detected almost everywhere on the Earth. The coherence spectrum of these two signals is equal to 1 in a frequency range from 0.1 to 1 Hz.

At the working day time (7 a.m.–5 p.m.), human activity leads to significant increase of the vibration amplitudes in the range of 2–100 Hz. Because of these high frequency components, the probe signals look like a white random noise. Consequently, the microseismic waves are not seen.

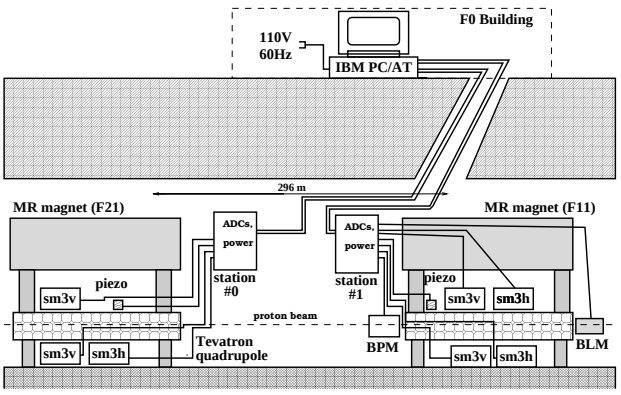

FIG. 2. Measurements in the main ring tunnel. The Tevatron ring is located under the main ring magnets.

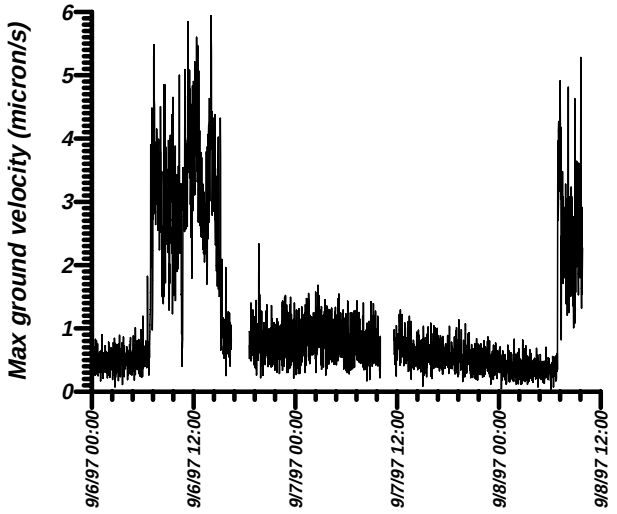

FIG. 3. Saturday, September 6–Monday, September 8, 1997 record of maximum vertical ground velocity at the E4R building.

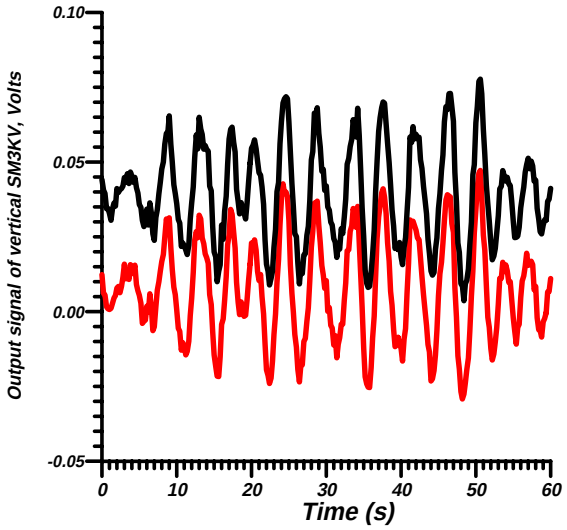

FIG. 4. (Color) Signals from two vertical SM3-KV geophones separated by 32 m (measured at night on September 17 and 18, 1997 on the E4R building floor).

Figure 5 presents the distribution of the displacement amplitudes of horizontal ground vibrations at E4R. Because the SM3-KV probe sensitivity falls down at periods longer than 10 s, we divided a many-hours-long record of the ground motion signal (started at 3:00 p.m. Wednesday, September 10) into 10 s intervals and calculated the amplitude of displacement in each interval by means of integration of the velocity signal. The distribution of those amplitudes is flat up to 0.2–0.3 μm; for larger amplitudes it rapidly goes down. The distribution function is non-Gaussian. One can fit the probability density of the displacement at the E4R building by the function

$$dW/dx \approx \frac{\text{const}}{a_{\min}[1 + (x/a_{\min})^2]^{\alpha/2}}. \qquad (5)$$

For the horizontal amplitude in Fig. 5, one has const $\approx$ 1, $a_{\min} \approx 0.4$ μm, and $\alpha \approx 2.7$. Corresponding probability that over a 10 s interval the displacement will occur with amplitude more than $x \gg a_{\min}$ is equal to

$$W \approx \frac{\text{const}}{\alpha - 1}\left(\frac{a_{\min}}{x}\right)^{\alpha-1}. \qquad (6)$$

Such a distribution can be very useful for the determination of parameters of the feedback system to control the closed orbit in accelerators. The distribution can help to estimate the probability of very large relative displacements of the magnets. Using only rms values without knowledge of the distribution, one cannot predict these large amplitude events.

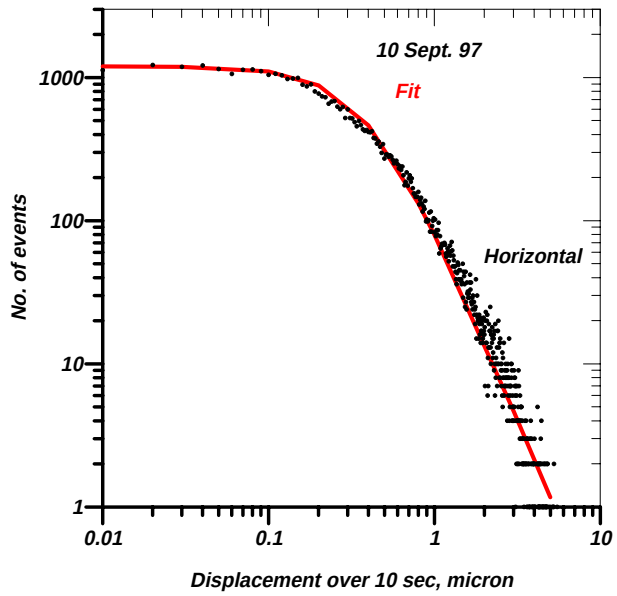

FIG. 5. (Color) Distribution of horizontal ground displacements over 10 s intervals.

The vibration measurements in the Tevatron tunnel have been done at Sector F11 (not far from the Tevatron RF station and the E4R building) and Sector F21, some 300 m apart. The computer was located on the surface in the F0 building. Seven SM3-KV probes (four vertical and three horizontal) and two vertical piezoaccelerometers were used. The layout of the experiment is shown in Fig. 2.

Station 0 is placed at a distance 296 m from station 1. The station 0 digitizes the signals from one vertical and one horizontal SM3-KV probe on the floor of the tunnel at F21 and from vertically oriented piezoaccelerometer and vertical and horizontal SM3-KV geophones on the Tevatron quadrupole magnet.

Station 1 digitizes the signals from four SM3-KV geophones (vertical and horizontal on the quadrupole magnet at F11 and vertical and horizontal on the tunnel floor nearby), one piezoaccelerometer placed on the same magnet, and, additionally, from a beam position monitor and a beam loss monitor.

Recording vibration signals in the Tevatron tunnel with 5 Hz sampling frequency, we observed little day–night variation of the maximum tunnel floor motion amplitude. Figure 6 presents the maximum vibration amplitude recorded from 3:30 p.m. September 3, 1997 until about 7:30 a.m. the next day (compare it to similar Fig. 3 for E4R site).

PSDs of vibrations of the F11 magnet, the tunnel floor, and at the E4R site are compared in Fig. 7. They are almost the same at frequencies of 5–30 Hz. At frequencies below 5 Hz and above 30 Hz, the magnet PSD is 10–100 times that of the floor. The "microseismic waves" demonstrate themselves as a broad peak near 0.2 Hz in the E4R spectrum. One can also see that below 5 Hz and above 20 Hz the vibration amplitude at the tunnel is higher than on the surface at night. Supposedly, at high frequencies the amplitude is higher due to the technical equipment (water and helium pipes, power cables, magnets themselves,

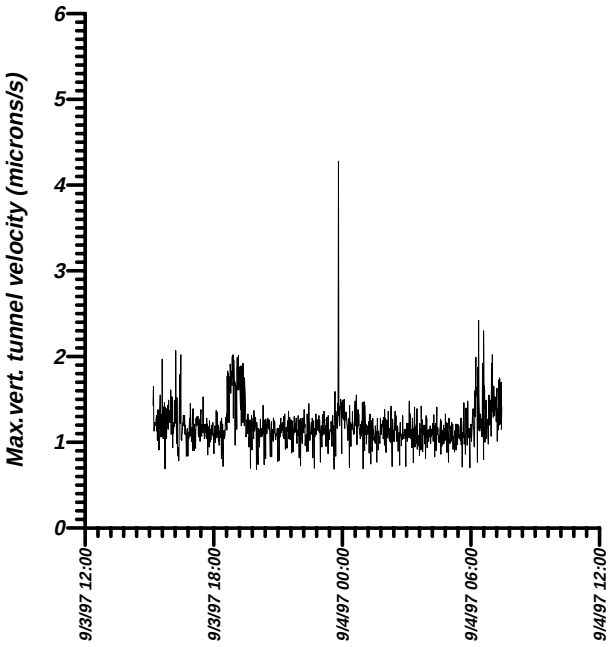

FIG. 6. Vibration amplitudes in the tunnel of the Tevatron over 16 h starting 3:30 p.m. September 3, 1997. The main ring and the Tevatron ring are operating.

etc.) in operation inside the tunnel. At frequencies around 1 Hz and lower, the main contribution is possibly due to strong mechanical distortions of the magnets during the main ring acceleration cycle (about 3 s) and the Tevatron acceleration cycle (about 60 s in fixed target operation).

Figure 8 presents results of the coherence measurements. As seen, the correlation between two vertical SM3-KV is very close to one in the frequency range from 0.1 to 100 Hz when the probes are placed in the E4R building side by side. At the distance of 62 m the coherence is near 1 only at microseismic and around 0.8 Hz peaks, then it rapidly falls to 0 at 50–100 Hz. For comparison, we present coherence of the Tevatron floor vertical motion measured with two SM3-KV probes separated by 296 m. The coherence is practically zero for all frequencies higher than 0.3 Hz. Except technological noise frequencies, the coherence tends to decrease very fast with an increase of the distance between probes.

The coherence spectra between the beam orbit and the magnet and between the beam orbit and the tunnel floor motion are presented in Fig. 9. One can see that the orbit correlates well with the floor only at low frequency 0.1 Hz, while some excessive but small coherence exists at 2–4 Hz. The beam orbit correlates with the quadrupole magnet motion at frequencies of 0.2–2 Hz. One possible origin of such coherence may be related to the 3 s accelerating cycle of the main ring, which mechanically affects closely located Tevatron magnets and produces an impact on the Tevatron beam via stray magnetic fields at harmonics of 1/3 Hz.

The closed orbit distortions are caused by the displacements of all magnetic elements along the circumference of the Tevatron. The strong coherence between the magnet and beam vibrations means that there is a common source of vibration along the whole accelerator ring. For example, several remarkable peaks in the orbit–magnet coherence occur at 4.6, 9.2, 13.8 Hz, etc., at the Fermilab site specific frequencies caused by the Central Helium Liquefier plant operation [8].

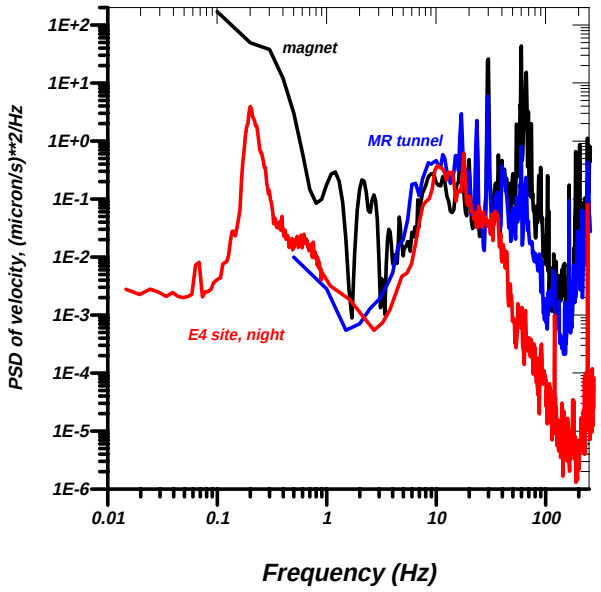

FIG. 7. (Color) Power spectral densities of vertical vibrations of the Tevatron quadrupole magnet (upper curve), the main ring tunnel floor, and on the surface at E4 (lower curve).

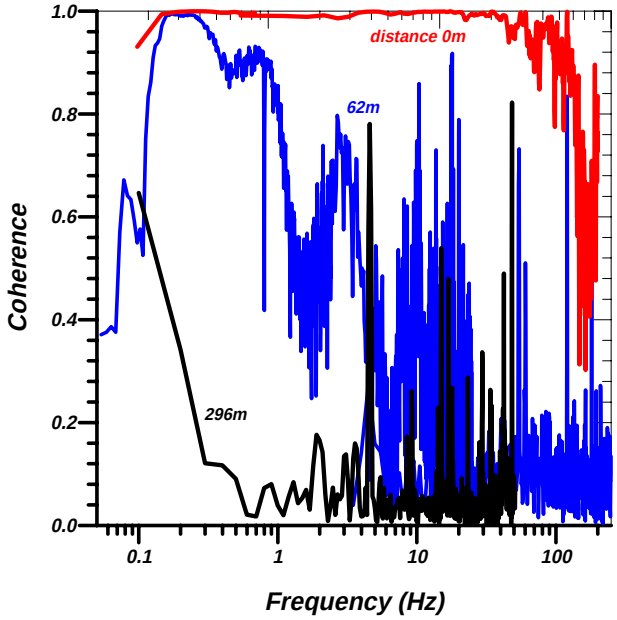

FIG. 8. (Color) Coherence of vertical ground motion signals measured by probes 0 and 62 m apart in E4R and 296 m apart in the Tevatron tunnel.

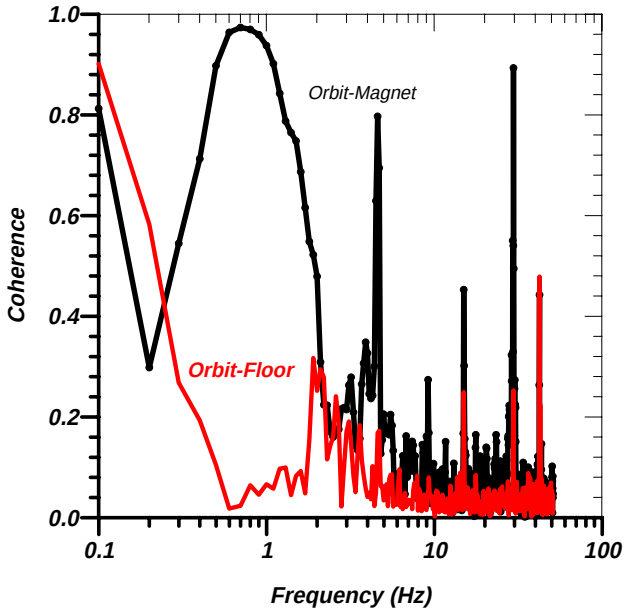

FIG. 9. (Color) Coherence between signals of the vertical Tevatron beam orbit motion and the F11 magnet vibrations (marked line) and between the orbit and the tunnel floor.

IV. MEASUREMENTS IN DEEP TUNNELS

Specific locations for possible Fermilab future colliders have not yet been chosen. There is also no definite requirement to be located within the Fermilab National Accelerator Laboratory site. For the purposes of radiation safety and tunnel stability, deep tunnels in the Illinois dolomite layer are alternative. This several-hundred-feet-thick layer is considered as moderately hard and stable. Details of the Illinois geology can be found elsewhere [9].

We studied seismic vibrations at two points of the Illinois dolomite layer. The first is a 250 ft deep mine (Conco Mine-Western Stone Co., North Aurora, IL; about 500 ft above sea level) located about 5 miles northwest of Fermilab. We carried out measurements there October 3–6, 1997. We refer to this data as "Aurora."

The second location is a 300 ft deep tunnel of the Metropolitan Water Reclamation District of Greater Chicago (MWRDGC) about 30 miles east of Fermilab in the Chicago suburb of Hodgkins, IL. It is near ($<$0.5 mile) an active interstate highway (I-55) and very close to a stone quarry. The tunnel was constructed as a part of the TARP of the MWRDGC. Our measurements there took nine days, October 8–17, 1997.

Despite restricted access to both tunnels (due to blasting and stone production in the Aurora mine and the operation schedule of the pumps of the MWRDGC), data acquisition was almost continuous, except for occasional few-hour periods for the data control, primary analysis, and relocation of the seismic probes for various experiments, e.g., for correlation measurements at different distances.

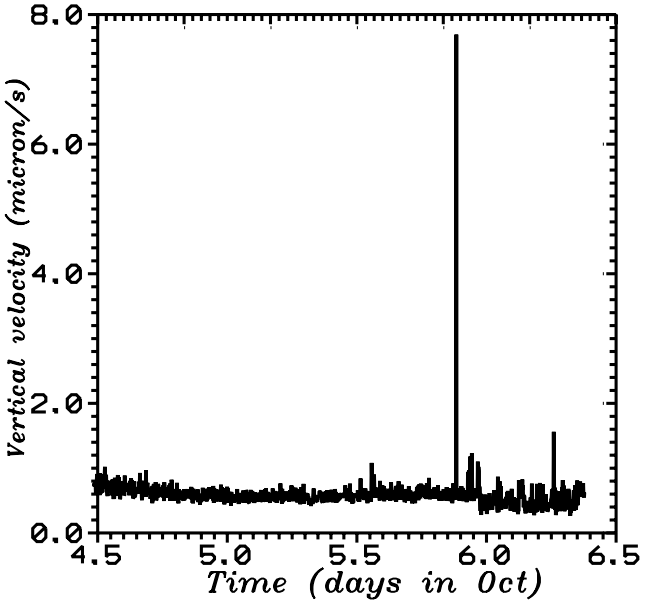

FIG. 10. Maximum ground velocity in the Aurora mine.

Figures 10 and 11 show long-term records of the maximum velocity detected in Aurora and TARP, respectively. Both are made with 10 Hz sampling frequency and 2 Hz low-pass filters. One can see that the amplitude was almost constant in the Aurora mine from noon on Saturday, October 4 until Monday morning, October 6. The main component of the signal is due to the microseismic waves and shows slight variations. Contribution of man-made noises was small because of the depth of the mine, low-pass filtering, and quiet weekend time when no powerful machinery worked in the mine. The lone peak in the Aurora mine record at about 10 p.m. on October 5

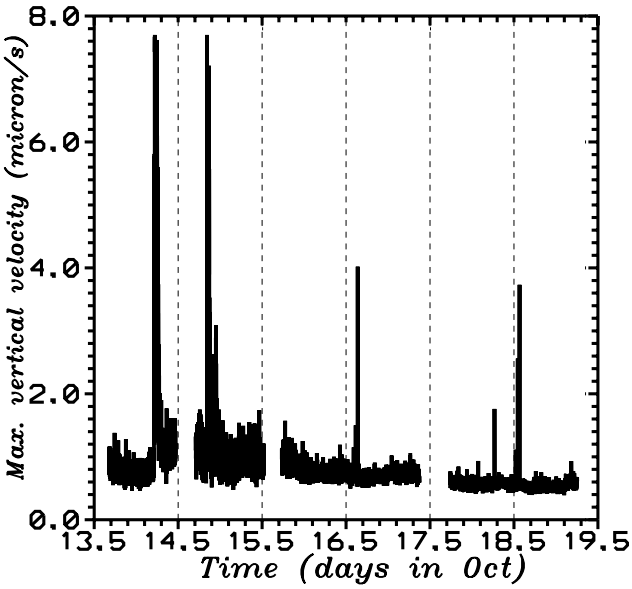

FIG. 11. Maximum ground velocity in the TARP shaft.

appeared when a superintendent of the mine came to check the equipment and passed nearby.

In contrast, the record made in the TARP shaft shows significant variations over several days. First, two long-lasting and significant perturbations are seen at about 5 a.m. on October 14, 1997, and at about 8:15 p.m. the same day. They are identified as 20–40 s period waves from powerful distant earthquakes: a magnitude 6.5 event in the Fiji island region and a magnitude 6.8 earthquake near the coast of central Chile. These waves traveled about 20–30 min before reaching Chicago. Figure 12 demonstrates the second of the earthquakes in more detail. It is a long-lasting (few hours) series of primary and secondary waves and aftershocks. One can see that the ground motion amplitude is of the order of 10–25 μm.

Blasting in the quarry near the TARP shaft produces short (about 1 min long) pulses of high-frequency (5–15 Hz) waves with relatively small amplitudes of about 0.1 μm or about 4 μm/s maximum velocity. Two of these events are seen in Fig. 11 at about 4:00 p.m. on October 16 and at 1:40 p.m. on October 18. Other short peaks in Fig. 11 are probably due to man-made activity in the TARP shaft (from time to time workers went down on a heavy elevator and worked near our detectors). It is interesting to note that the background level of the maximum ground velocity in Fig. 11 varies substantially—it is much larger on Monday, October 13 and smaller in the evening of Friday, October 17 and Saturday, October 18. We think the reason can be residual excitation from on-surface sources (highways, roads, quarry operation, etc.), which are usually less active on weekends.

Power spectral densities of the ground velocities measured in the Aurora mine and in the TARP shaft are presented in Fig. 13 in comparison with the Tevatron quadrupole magnet vibration PSD. These spectra cover five decades of frequency band from 0.005 to 280 Hz and are obtained with different probes and with different sampling rates (besides different places and different times). For example, the TARP curve (solid line) consists of spectra measured by the STS-2 vertical probe (from 0.005 to 0.1 Hz), by the SM3-KV geophone (from 0.1 to 120 Hz), and by the Wiloxon piezoprobe (from 120 to 280 Hz). The Aurora data (dashed line) show no vibration spectra above 120 Hz—the motion is too small to be detected by the piezoaccelerometers.

One can see that the Aurora mine is the quietest place of the three. Some technologically related peaks are seen in the Aurora PSD only in the 60–120 Hz range. We believe that it is due to lighting transformers in the tunnel. Below 0.5 Hz the spectral density in the Aurora mine and in the TARP tunnel are about the same and are mainly due to microseismic waves. Above 2 Hz, the TARP PSD is 20–800 times the Aurora mine PSD. A noisier environment on the surface and more technological equipment in the tunnel itself are probable reasons for two very broad peaks in the TARP spectrum at 5 Hz and around 25 Hz, respectively (as damping decrement of the ground grows with frequency). Finally, the Tevatron quadrupole spectrum consists of many peaks (4.6, 9.2, 20, 60 Hz, etc.) and is much noisier (as we discussed above, due to the Tevatron equipment) than the others above 10 Hz.

Integration of these spectra accordingly to

$$\sigma_x(f) = \int_f^\infty S_x(f)\,df = \int_f^\infty S_v(f)\,\frac{df}{(2\pi f)^2} \qquad (7)$$

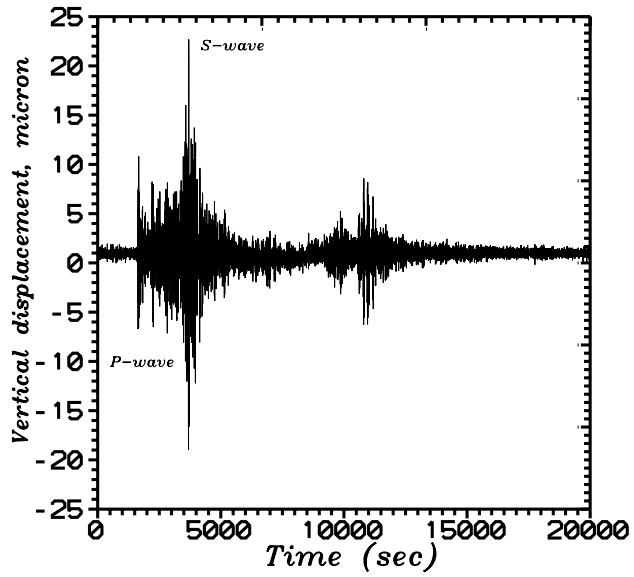

FIG. 12. Earthquake waves. Record starts at 7:45 p.m. October 14, 1997.

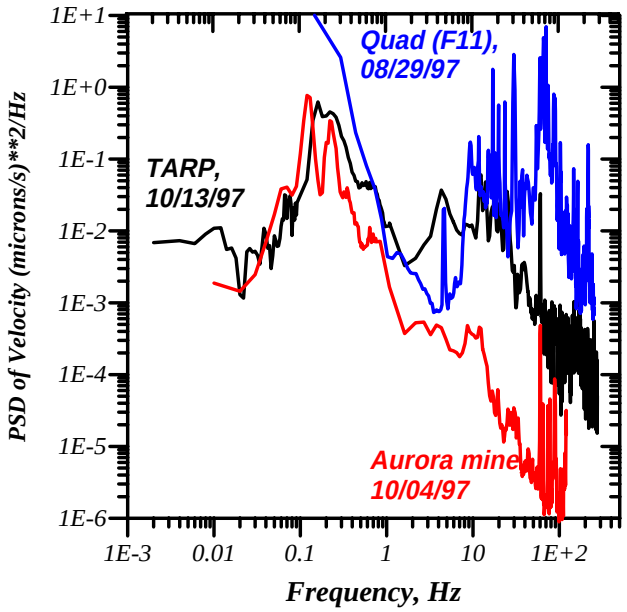

FIG. 13. (Color) Spectra of ground motion in the Aurora mine, the TARP tunnel, and the Tevatron magnet vibrations

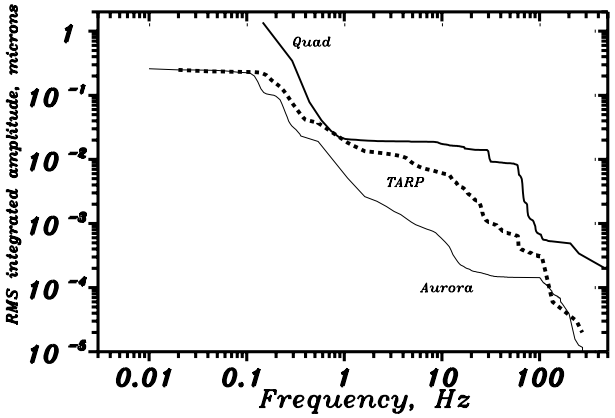

FIG. 14. Integrated rms ground motion amplitude.

[here $S_v(f)$ is the PSD of velocity and $S_x(f) = S_v(f)/\omega^2$ is the PSD of displacement] gives us the rms amplitudes of vibrations presented in Fig. 14. One can see that the amplitudes in the deep tunnels are about 0.3 μm at frequencies ~0.5 Hz and below, while above 100 Hz they are less than 0.1 nm $= 10^{-4}$ μm. Motion of the quadrupole is several times larger.

Many figures presented in this paper refer to vertical ground motion. In fact, the forces in the ground are much stronger than the gravity and, in principle, there must be no significant difference between the vertical and the horizontal ground noises. Figure 15 presents the spectra of the vertical and horizontal movements in the TARP shaft. They are rather similar and the PSDs are the same within a factor of 3–5 over the wide frequency range of 0.06–100 Hz.

Figure 16 shows real and imaginary parts of the correlation spectrum $C_{x_1x_2}(f)$ of signals from two vertical SM3-KV geophones placed 75 m apart in the TARP shaft. Each of the curves is an average over 200 measurements

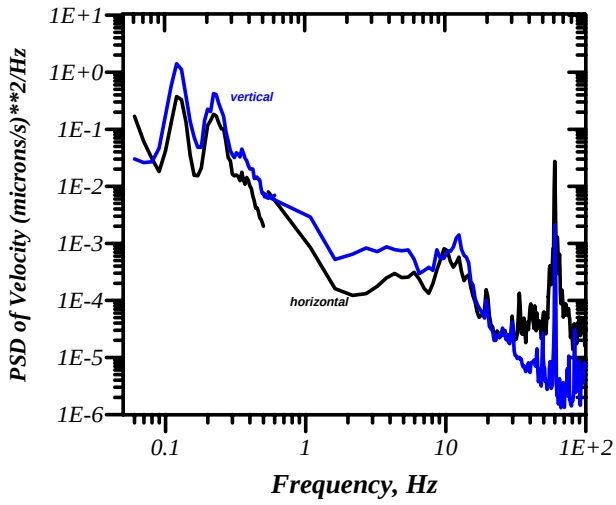

FIG. 15. (Color) Comparison of vertical and horizontal ground motion spectra. TARP measurements.

that gives an estimate of the statistical error of about 0.1. The first remarkable feature of the data is that at frequencies below 100 Hz the real part is much larger than the imaginary one. The latter is almost 0 below 10 Hz, while the real part performs some damped oscillations with the frequency increase. Such a behavior is close to the prediction of the model in which the vibration sources are uniformly and continuously distributed over ground surface and generate waves at all frequencies without any phase correlation; see, e.g., [6]. Under these assumptions, the correlation spectrum between signals detected in two points L meters apart is equal to

$$\mathrm{Re}\, C(f) = J_0[2\pi L f/v(f)], \quad \mathrm{Im}\, C(f) = 0, \quad (8)$$

where $v(f)$ is the wave propagation velocity and $J_0(x)$ is the 0th order Bessel function. In Fig. 16 we present the fitting curves with parameters $L = 75$ m and $v(f)$ [m/s] $= 3800 - 4f$ [Hz].

The spectra of coherence, i.e., $|C(f)|$, between two vertical SM3-KV geophones in the TARP tunnel separated by 8, 21, 43, and 75 m are presented in Fig. 17.

One can make the general conclusion that the coherence goes down not only with increase of the frequency f but with increase of the distance between two points as well. In particular, the tunnel vibrations of two points 75 m apart at frequencies of 90–230 Hz can be considered as uncorrelated since the coherence is small. Note that at the local ac power frequency of 60 Hz, the coherence is high due to powerful and correlated noise contribution.

V. DISCUSSION AND CONCLUSION

We can now compare measured ground vibrations with the Fermilab future collider requirements outlined in

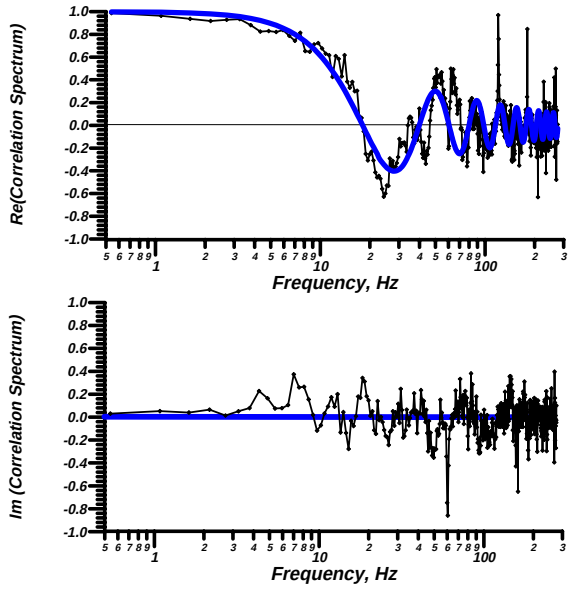

FIG. 16. (Color) Real and imaginary parts of correlation spectra measured in the TARP shaft at a distance of 75 m between probes and fit accordingly to the random source model.

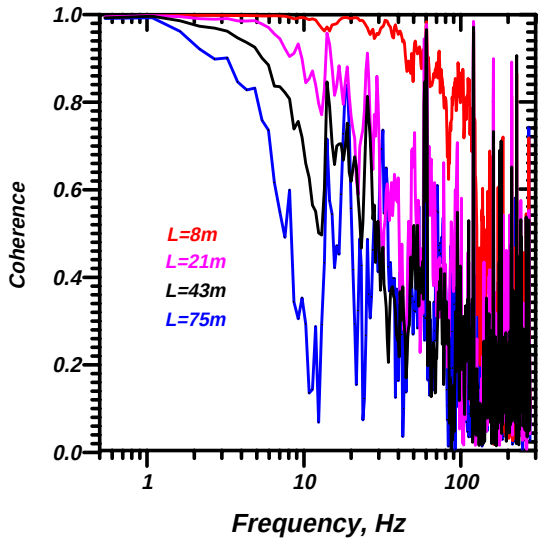

FIG. 17. (Color) Coherence of the ground motion vs distance. TARP measurements.

Table I. Figure 18 presents integrated vibration amplitudes in the Aurora mine and on top of the Tevatron quadrupole. Other curves are for the tolerances: for the X-band linear collider it is the ground motion which causes 1.5% luminosity degradation accordingly to Ref. [6]. We would like to emphasize that the tolerances for other than the X-band LCs can be much less stringent if larger bunch spacing allows one to implement a bunch-by-bunch trajectory correction feedback system. The muon collider requirement is presented by the rms amplitude of focusing magnets that leads to beams separation of about 10% of the rms beam size at the interaction point. The VLHC tolerance consists of two parts [7]. At frequencies below 10 Hz the curve shows the vibration amplitude that causes the beam orbit vibration amplitude about 10% of the rms beam size. Above 90 Hz the line corresponds to requirements on the rms transverse emittance growth less than 0.1 πmm · mrad/5 h without (solid line) and with feedback systems to damp excited betatron oscillations (dashed line; feedback allows one to ease the ground motion tolerances some 10 times or more depending on the beam parameters [5]). One can see that the Aurora mine amplitudes are below all the tolerances, although close to the VLHC ones around 90–120 Hz. In contrast, vibrations of the Tevatron quadrupole are potentially very dangerous for all three machines at frequencies below 20–60 Hz (orders of magnitude excess), and several times above the VLHC requirement above 70 Hz.

Figure 19 shows the results of the emittance growth simulations for the VLHC. They were made under the assumption that movements of all 2200 quadrupoles in the collider are independent. The beam is represented by some hundred macroparticles oscillating in the focusing lattice with somewhat different frequencies around the mean tune of $\nu = 0.265$. The motion of the quadrupole magnets is taken from a file with a real record of ground vibrations made with a sampling frequency equal to the VLHC revolution frequency of 554 Hz (see details of the method in Ref. [10]).

Figure 19 shows the evolution of the emittance increase with two 10 min long files with motion of the Tevatron quadrupole magnet (upper curve) and vibrations of the Aurora mine (lower curve). The emittance growth rate corresponding to the Tevatron quadrupole curve is about 1.2π mm · mrad/5 h, or, equivalently, it is more than double that of the initial emittance of 1π mm · mrad over the beam lifetime. The emittance growth rate under the conditions of the Aurora mine will be as low as 0.04π mm · mrad/5 h, i.e., 4% of the initial emittance over the same 5 h.

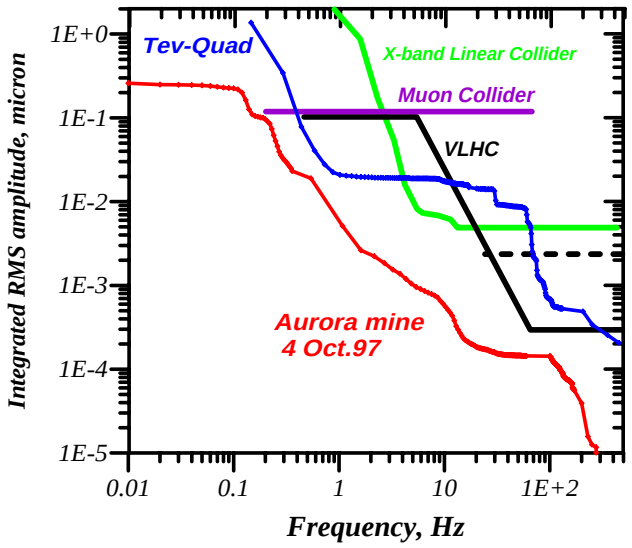

FIG. 18. (Color) Comparison of the measured ground and quadrupole vibration amplitudes with tolerances for the muon collider, X-band linear collider, and the VLHC.

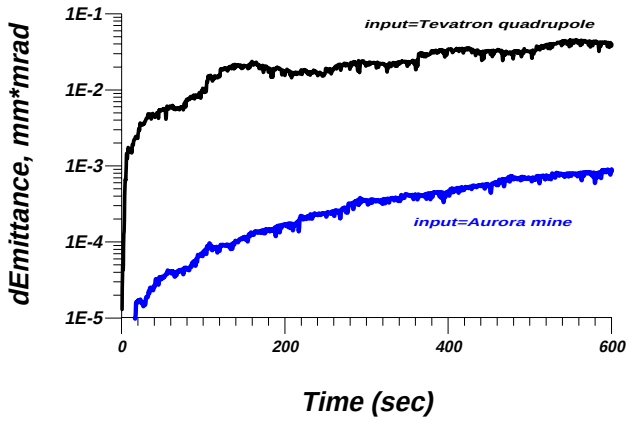

FIG. 19. (Color) The VLHC emittance growth simulations with two data inputs: Tevatron quadrupole vibrations (upper line) and the Aurora mine tunnel (lower line) vibrations as input.

We have to note that, in general, accelerators are relatively "noisy" sites because of their technical noises. We compare our data with previous measurements at accelerator facilities in Fig. 20. It presents the PSDs of ground velocity $S_v(f) = S_x(f)(2\pi f)^2$ measured in the Aurora mine (marked as FNAL) and in the tunnels of the SLC (SLAC) [6], HERA [11], KEK [12], LEP (CERN) [13], and the so-called "New Low Noise Model" [14]—a minimum of geophysical observations worldwide. One can see that the PSDs measured at accelerators are well above the "low-noise" spectrum. At the same time, vibrations in HERA, which is located under the populated area in the city of Hamburg, are somewhat larger than in the other tunnels.

Finally, we summarize the results of our studies.

(a) Ground vibrations have been measured at the FNAL site and in deep tunnels outside in wide frequency band from a few hundredths of a hertz to several hundred hertz. We have observed that vibrations above 1 Hz are well affected by cultural noises, which vary significantly in time, and also strongly depend on location and depth, while below 1 Hz the main contribution to the ground motion comes from natural sources and performs slow temporal variations.

(b) A comparison of on-surface and underground sites have shown that levels of vibrations are typically smaller in deep tunnels. Effects due to on-surface noise sources are less seen in the deep tunnels, though visible. Amplitudes of horizontal and vertical vibrations are found to be about the same in the frequency band of the experiments.

(c) During the daytime and on the Fermilab site, neither the E4 building (on surface) nor the main ring tunnel are quiet enough for future colliders, especially for the VLHC. The ground motion at night in the main ring tunnel with two accelerators under operation is not too different from its daytime levels, while the vibration amplitude at the E4 becomes about or less than the VLHC tolerance.

(d) The maximum amplitudes are observed for the motion of the Tevatron quadrupole magnets when the Tevatron and the main ring accelerators were operating. It was somewhat larger than the motion of the tunnel floor nearby. Careful engineering of mechanical supports, of vacuum, power, and cooling systems should be an important part of research and development efforts to decrease the level of vibrations in any other future collider.

(e) In deep tunnels in the Illinois dolomite (Aurora mine and the TARP shaft), we observed vibrations below the tolerances for all the collider projects. As the amplitudes of ground vibrations are smaller at higher frequencies, we propose to operate the VLHC at a higher fractional part of the tune because it concludes in higher resonance betatron frequencies.

(f) One should give proper attention at the stage of the design and construction of the large accelerators to decrease the level of technical vibration, then it can be possible to obtain vibration amplitudes 10–100 times smaller than in the Tevatron now, and closer to what we detected in the deep tunnels. It is necessary to place potential sources of vibrations as far away as possible from the accelerator ring and/or to damp vibrations at their origin. From this point of view, it seems very useful to have a seismic monitoring system for future colliders.

(g) Investigations of spatial characteristics of the fast ground motion have shown that above 1–4 Hz the correlation significantly drops at dozens of meters of the distance between points. Therefore, the displacements of different magnetic elements of the accelerator (which will be spaced by hundreds of meters) can be regarded as uncorrelated except for characteristic frequencies of technical devices producing the vibrations along the whole ring (electric power, water, nitrogen and helium systems, etc.). The model of uniformly distributed random sources satisfactorily describes the ground motion spatial correlation spectra.

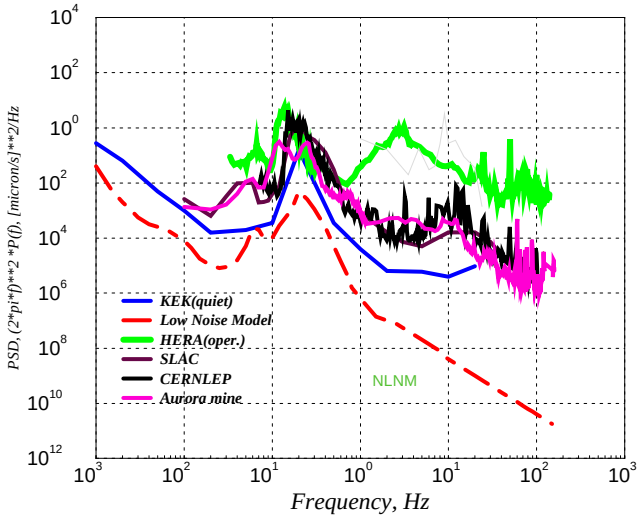

FIG. 20. (Color) Ground motion spectra at different accelerator sites and the USGS new low-noise model.

ACKNOWLEDGMENTS

We acknowledge the help of many people during the preparation of the apparatus and the measurements: Anatoly Medvedko (BINP), Frank Nezrick, Mark Averett, Dean Still, Ken Koch, Rupe Crouch, Marv Olson, and Jim Zagel (FNAL). We are indebted to Chris Adolphsen (SLAC) and Jim Norem (ANL) for cooperation in providing us with two STS-2 seismometers. Measurements out of the Fermilab site would not have been done without the help of Mike Dunn of the Conco-Western Stone Co., Hugh McMillan, Gerry Garbis, Bob Kuhl, Tom Nolan, and Al Yescenski of the Metropolitan Water Reclamation District of Greater Chicago, and Mike Ralls of FNAL. We sincerely acknowledge their cooperative attitude to

our seismic investigations. We also thank Dave Finley, Ernie Malamud (FNAL), and Nikolay Dikansky (BINP) for their steady interest in seismic studies and support of this activity. The Fermi National Accelerator Laboratory is operated by the Universities Research Association, Inc., under contract with the U.S. Department of Energy.

[1] G. E. Fisher, in *Physics of Particle Accelerators*, edited by Melvin Month and Margaret Deines, AIP Conf. Proc. No. 153 (AIP, New York, 1985).
[2] V. Shiltsev, in *Fifth European Particle Accelerator Conference, Barcelona, 1996* (Institute of Physics Publishing, Bristol, Philadelphia, 1996).
[3] $\mu^+\mu^-$ Collider: A Feasibility Study, Report No. FNAL-Conf-96/092, BNL-52503, LBNL-38946, 1996, edited by J. Gallardo.
[4] G. W. Foster and E. Malamud, Report No. FNAL-TM-1976, 1996.
[5] V. Lebedev *et al.*, Part. Accel. **44**, 147 (1994).
[6] The NLC Design Group, Report No. SLAC-R-0485, Appendix C of NLC ZDR, 1996.
[7] V. Shiltsev, Report No. FNAL-TM-1987, 1996.
[8] C. Moore, *Proceedings of the 4th International Workshop on Accelerator Alignment* (KEK, Ibaraki, Japan, 1995), p. 119.
[9] P. C. Heigold, Illinois State Geological Survey (1990).
[10] V. Shiltsev and V. Parkhomchuk, Report No. SSCL-639, 1993.
[11] V. Shiltsev *et al., Proceedings of the 1995 IEEE Particle Accelerator Conference, Dallas, Texas* (IEEE, New York, 1995), pp. 2078, 3424.
[12] S. Takeda and M. Yoshioka, KEK Report No. 95-209, 1996.
[13] V. Jouravlev *et al.*, Report No. CERN-SL/93-53, 1993; Report No. CLIC-Note-217, 1993.
[14] J. Peterson, USGS Open-File Report 93-322, 1993.